# Influences of Mo/Zr minor-alloying on the phase precipitation behavior in modified 310S austenitic stainless steels at high temperatures

Donghui Wen[a], Beibei Jiang[a], Qing Wang[a],*, Fengyun Yu[a], Xiaona Li[a], Rui Tang[b], Ruiqian Zhang[b], Guoqing Chen[a], Chuang Dong[a]

[a] Key Laboratory of Materials Modification by Laser, Ion and Electron Beams (Ministry of Education), School of Materials Science and Engineering, Dalian University of Technology, Dalian 116024, China
[b] Science and Technology on Reactor Fuel and Materials Laboratory, Nuclear Power Institute of China, Chengdu 610213, China

## ARTICLE INFO

## ABSTRACT

High-Cr/Ni austenitic stainless steels (ASSs) have attracted more attention as fuel cladding materials of super-critical water reactors due to their excellent comprehensive properties. In order to further improve their microstructural stability at high temperatures, the present work investigated systematically the influences of Mo/Zr contents and Zr/C ratios on the phase precipitation behaviors and mechanical properties of modified 310S ASSs. The designed alloy ingots were hot-rolled, solid-solutioned at 1423 K for 0.5 h, stabilized at 1173 K for 0.5 h, and then aged at 973 K for different hours. The microstructure and precipitated phases at different heat-treatment states were characterized with OM, SEM, EPMA and TEM, respectively. All the results indicated that the excess addition of Mo and Zr and the inappropriate Zr/C ratios would promote the formation of $Cr_{23}C_6$, G-$Ni_{16}Si_7Zr_6$ and $(Ni,Fe)_{23}Zr_6$ phases, resulting in the σ phase precipitation at the early stabilization stage. Furthermore, the formation mechanism of σ phase was discussed. The effects of the precipitated phases on the mechanical properties of alloys were then studied. It was found that the Fe-22Ni-25Cr-0.046C-0.37Mo-0.35Zr (wt%) alloy with appropriate Mo content and Zr/C ratio of 1/1 exhibits the best microstructural stability and good tensile mechanical property, in which only a few σ particles are precipitated from the matrix even after aging at 973 K for 408 h.

## 1. Introduction

Austenitic stainless steels (ASSs) would be potentially applied into the super-critical water reactors (SCWRs) as fuel cladding materials and core components under the extreme conditions (573–923 K/25 MPa/ neutron irradiation), as they exhibit higher creep strength, better corrosion- and oxidation-resistance than the commercial zirconium alloys [1–4]. Specially, such ASSs contain high Cr and Ni contents of (20–25)Cr-(20–25)Ni (the numbers in front of elements represent the weight percent, wt%), such as 310S (Fe-25Cr-20Ni-0.08C), HR3C (Fe-25Cr-20Ni-0.4Nb-0.1C-0.2N), and NF709 (Fe-20Cr-25Ni-0.08C-1.5Mo-0.3Nb-0.1Ti-0.15N), exhibiting better radiation-induced fragility resistance in comparison with Ni-based superalloys [5–9].

To guarantee the service performance, the microstructural stability of these ASSs is of utmost importance. The main cause is that some harmful phases, like $Cr_{23}C_6$ (cF-$C_6Cr_{23}$ type), FeCr (tP-CrFe type, abbreviated as σ), $Cr_6Fe_{18}Mo_5$ (cI-Mn type), and Laves phase $Fe_2$(Mo/ Nb) (hP-$Zn_2Mg$ type), could be precipitated inevitably from the

austenitic matrix after a long-term aging at 873–1173 K, as a final result of an embrittlement of materials [10–13]. For instance, a large amount of coarse $Cr_{23}C_6$ and σ phases were precipitated from the austenite matrix in 310S ASS after aging at 973 K for 1 h due to the high Cr content, resulting in a drastic drop of impact toughness and corrosion resistance [14,15]. Although strong carbide-forming elements of Nb and Ti were used to minor-alloy the 310S, the microstructural stability of the modified ASSs, such as HR3C and NF709, have not been improved obviously because an abundant amount of $Cr_{23}C_6$ and σ particles were still existed after a long-term aging at 923–1073 K [16–18]. A recent study [19] on the Mo (0.51 wt%) and Zr (0.59 wt %) co-alloying of 310S with a super-low C (0.034 wt%) indicated that the σ precipitation could be retarded and the microstructural stability was then improved on some extent in comparison with those of HR3C and NF709 ASSs. However, the coarse σ particles still appeared after a long-term of 500 h aging at 823 K. Moreover, the types of other precipitated phases in this Mo/Zr-modified ASS have not been identified clearly due to the complex interactions induced by the multi-

component co-alloying [19].

Intrinsically, the minor-alloying elements are of utmost importance to the property improvement of stainless steels. For instance, the element Mo could enhance the pitting resistance and solid-solution strengthening [20–22]. As a strong carbide-forming element, Zr often tends to form ZrC with C to avoid the formation of $Cr_{23}C_6$, similar to Nb, Ta and Ti [23–25]. However, the property improvement is always accompanied by the precipitation of some harmful phases at high temperatures. It might be caused by the unreasonable matching among minor-alloying elements from the viewpoint of chemical composition [10–25]. Actually, the influences of the types and contents of minor-alloying elements on the phase precipitation behavior in the modified 310S ASSs has not been investigated systematically by far. Therefore, in the present work, the C content is decreased below 0.05 wt% for the inhibition of $Cr_{23}C_6$, and the basic alloying elements of Cr and Ni are still maintained at 25Cr-22Ni. Zr and C are tuned simultaneously to satisfy the Zr/C ratios of 1/1 and 3/1 (molar proportion), respectively, in which the 1/1 ratio is a stoichiometric matching for ZrC carbide and the 3/1 ratio means the excess addition of Zr. Mo is also added to enhance the matrix by the solid-solution strengthening mechanism. Four alloys with different element contents, as seen in Table 1, are then designed to investigate the influences of Mo and Zr contents and Zr/C ratios on the phase precipitation behavior from the austenitic matrix, i.e., microstructural stability of alloys at high temperatures.

## 2. Experimental

The designed alloy compositions were listed in Table 1, in which the S0 alloy represents the base alloy 310S with a low C content of 0.046 wt %. The S1 and S2 alloys contain a same Zr/C ratio of 1/1 with a Zr content of 0.35 wt%, but with different Mo contents. Thereafter, the S1 and S2 alloys are marked with 0.73Mo/0.35Zr and 0.37Mo/0.35Zr, respectively. The S3 alloy is marked with 0.73Mo/0.52Zr, where the Zr/C ratio is 3/1, i.e., a relatively-higher Zr content is added into the alloy in combination with a super-low C of 0.023 wt%. In addition, Si (0.40 wt%) and Mn (0.78 wt%) are intended to be added into these alloys to imitate the impurity contents in such kind of ASSs.

These four alloy ingots with about 60 g were prepared by a vacuum arc-melting furnace. The purities of the raw metals are 99.99 wt% for Fe, Ni, Zr, C and Si, 99.5 wt% for Mo, and 99.9 wt% for Cr and Mn, respectively. Before melting, the vacuum of the furnace was controlled below $6 \times 10^{-3}$ Pa, and the melting process were protected by the argon atmosphere with a purity of 99.999%. These alloy ingots were melted repeatedly at least five times for composition homogeneity, in which the mass loss could be controlled below 0.1 wt%. They were homogenized at 1423 K for 0.5 h and then hot-rolled for several times with a total deformation of 80%, in which the rolled samples were reheated for 5 mins before each rolling. The hot-rolled plates with a thickness of about 1.4 mm were again solid-solutioned at 1423 K for 0.5 h plus water-quenching, and then stabilized at 1173 K for 0.5 h plus furnace-cooling. Finally, the stabilized plate samples were aged at 973 K for different time of 25 h, 50 h, 100 h, 200 h, 300 h, and 408 h, respectively.

Structural identification of alloy samples with different heat treatments were carried out by means of BRUKER X-ray diffractometer (XRD) with a Cu $K_\alpha$ radiation ($\lambda$ = 0.15406 nm). The microstructure

was observed using OLYMPUS optical microscopy (OM) and Zeiss Supra55 scanning electron microscopy (SEM) with an etching solution of 20% HF + 10% $HNO_3$ + 70% $H_2O$ (volume fraction). The elemental distributions were analyzed by SHIMADZU electron probe micro-analyzer (EPMA). The crystalline structures of precipitated phases were further identified by Philips Tecnai $G^2$ transmission electron microscopy (TEM), where the TEM samples were prepared by twin-jet electro-polishing in a solution of 10% $HClO_4$ + 90% $C_2H_5OH$ (volume fraction) at about 243 K. The statistical analysis of the volume fraction and size of precipitated particles at different heat-treatment states were measured from the SEM morphology images (at least 6 images) by using the Image-Pro Plus 6.0 software.

Uniaxial tensile tests of the stabilized and 408 h–aged samples were conducted on an 810 Material Test System (MTS) with a strain rate of $1*10^{-3}$/s at room temperature, in which the plate-shaped samples have a gauge size of 25.0*4.0*1.1 mm (length*width*thickness) and two tensile samples for each alloy were prepared. The fracture morphologies of these tensile samples were also observed with the SEM. Moreover, the micro-hardness tests of all the samples at different heat treatment states were conducted using a HVS-1000 apparatus with a load of 500 g for 20 s, where each alloy sample was tested at least for ten times.

## 3. Results

### 3.1. Microstructural characterization of solution- and stabilization-treated alloys

All the solid-solutioned plate samples of the alloys exhibit a single face-centered-cubic (FCC) γ austenitic structure, as seen in the XRD patterns (Fig. 1(a)). The SEM observations also verified the XRD results, as shown in Fig. 1(b), showing a typical morphology of austenitic
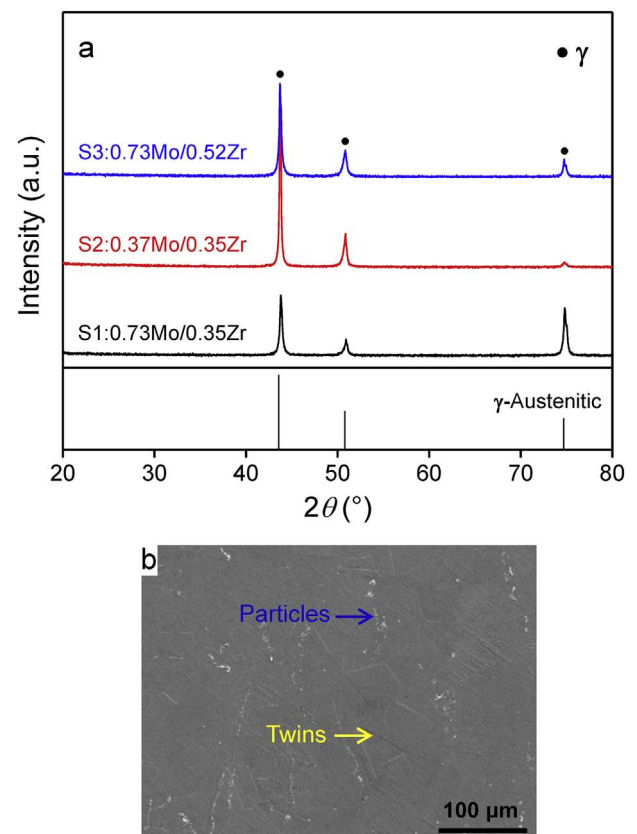


**Table 1**
Chemical compositions of the designed alloys (wt%).

| No. | Alloys | Ni | Cr | Mo | Zr | C | Si | Mn | Fe |
|---|---|---|---|---|---|---|---|---|---|
| S0 | 310S | 22.42 | 24.83 | | | 0.046 | 0.40 | 0.78 | Bal. |
| S1 | 0.73Mo/0.35Zr | 22.32 | 24.72 | 0.73 | 0.35 | 0.046 | 0.40 | 0.78 | Bal. |
| S2 | 0.37Mo/0.35Zr | 22.36 | 24.76 | 0.37 | 0.35 | 0.046 | 0.40 | 0.78 | Bal. |
| S3 | 0.73Mo/0.52Zr | 21.19 | 24.69 | 0.73 | 0.52 | 0.023 | 0.40 | 0.78 | Bal. |

**Fig. 1.** XRD patterns (a) and typical SEM morphology (b) of the solid-solutioned Mo/Zr modified 310S alloys.